Journal of Chemistry and Technologies, 2022, *30*(1), 60-68

Journal of Chemistry and Technologies

pISSN 2663-2934 (Print), ISSN 2663-2942 (Online).

journal homepage: http://chemistry.dnu.dp.ua

UDC 661.665

SYNTHESIS OF ZEOLITE FROM NATURAL CLAY AND RICE HUSK ASH TO LOWER THE BAND GAP OF TITANIA AS A PROMISING PHOTOCATALYST

Syukri*, Ahmad Fikri, Safni, Olly Norita Tetra

Department of Chemistry, Faculty of Mathematic and Natural Sciences, Andalas University

Abstract

In this study, we have utilized clay from Pariaman, Indonesia enriched with silica from rice husk ash to produce zeolite through a hydrothermal process. The resulting zeolite is then composited with the most common semiconductor photocatalyst, an anatase titanium oxide, to increase the semiconductor efficiency in terms of particle distribution and light sources activation. From X-Ray Fluorescence (XRF) measurement, it can be seen that the Si/Al mole ratio in the clay has been successfully increased from 1.8 to 2.0. These data are strengthened by the results of X-Ray Diffraction (XRD) analysis which shows the formation of zeolites of several types consisting of zeolite faujasite, P1, sodalite, X, and nu-6. When the synthesized zeolite is mixed with titania anatase, a composite is formed as evidenced by FTIR analysis with the appearance of Si-O-Si and Si-O-Al absorption bands for zeolite and Ti-O-Ti from titania. This zeolite has been shown to reduce the bandgap energy of titanium oxide after the two materials have been composited. Measurements with Ultraviolet-Visible Diffuse Reflectance Spectroscopy (UV-Vis DRS) showed that the TiO_2-anatase band gap decreased by about 20 %, from 3.20 to 2.56 eV allowing theoretically the composite to be considered as a promising photocatalyst.

Keywords: Clay; zeolite; semiconductor photocatalyst; composite; and band gap.

СИНТЕЗ ЦЕОЛІТУ З ПРИРОДНОЇ ГЛИНИ І ЗОЛИ РИСОВОГО ЛУШПИННЯ В ЯКОСТІ ПЕРСПЕКТИВНОГО ФОТОКАТАЛІЗАТОРА ДЛЯ ЗМЕНШЕННЯ ЗАБОРОНЕНОЇ ЗОНИ ДІОКСИДУ ТИТАНУ

Сюкрі, Ахмад Факрі, Сафні, Оллі Норта Тетра

Кафедра хімії, факультет математики та природничих наук, Університет Андалас, Падант, Індонезія

Анотація

У даному дослідженні збагачена кремнієм із золи рисового лушпиння глина з Паріаману, Індонезія, була використана для отримання цеоліту в результаті гідротермального процесу. Отриманий цеоліт був з'єднаний з найбільш поширеним напівпровідниковим фотокаталізатором, анатазним діоксидом титану, для підвищення ефективності напівпровідника з точки зору розподілу частинок і активації джерел світла. З вимірювань рентгенівської флуоресценції (XRF) видно, що мольне співвідношення Si/Al в глині було успішно збільшено з 1.8 до 2.0. Ці дані підкріплені результатами аналізу рентгенівської дифракції (XRD), який показує утворення цеолітів декількох типів - фоязиту, P1, содаліту, X, і nu-6. При змішуванні синтезованого цеоліту з анатазним діоксидом титану утворюється композит, про що свідчить аналіз FTIR з появою смуг поглинання Si-O-Si і Si-O-Al для цеоліту і Ti-O-Ti для діоксиду титану. Показано, що цей цеоліт зменшує енергію забороненої зони діоксиду титану після з'єднання двох матеріалів. Дослідження за допомогою ультрафіолетово-видимої спектроскопії дифузного відбиття (UV-Vis DRS) показали, що заборонена зона TiO_2-анатаза зменшилася приблизно на 20 %, з 3.20 до 2.56 еВ, що теоретично дозволяє розглядати композит як перспективний фотокаталізатор.

Ключові слова: глина; цеоліт; напівпровідниковий фотокаталізатор; композит; заборонена зона.

**Corresponding author: e-mail: syukridarajat@sci.unand.ac.id*

doi: 10.15421/jchemtech.v30i1.237739

Introduction

Waste of liquid and gaseous contaminants from organic compounds is one of the important problems around the world, because it damages natural ecosystems and also disrupts the environment. Common problems that often arise from this type of waste are water eutrophication, air and aquatic pollution, and disturbing environmental ecosystems[1]. Various studies have been developed to address this problem. Adsorption and ion exchange are methods that are often used in dealing with this problem, however, both of these methods have the disadvantage of being able to only absorb and exchange contaminants without any further degradation processes [2].

Recently, many researchers have conducted studies and research on more effective waste treatment called the Advanced Oxidation Processes (AOPs), one of which is the use of photocatalysts. The advantages of the photocatalytic method are that it is more efficient, economical and is able to completely eliminate contaminant compounds[3]. Recently, catalysts based on semiconductor materials are widely used for various applications. Transition metal oxide semiconductor photocatalysts have been applied intensively for waste treatment through advanced oxidation processes [4]. The semiconductor most commonly used in the degradation process is TiO_2 because it is relatively more economical, non-toxic, has a stable structure, and excellent catalytic properties compared to other metal oxide semiconductors [5].

In nature, TiO_2 is found in three crystalline forms consisting of anatase, rutile and brookite. In terms of photocatalytic activity, the anatase phase form is superior to the other two due to the high density of anatase crystal structure and its highest electrical conductivity[6]. The problem that still needs to be resolved is that the titania anatase band gap energy is relatively quite large around ~3.2 eV, so it is difficult to activate it with visible light. It makes its application difficult and uneconomical because ultraviolet light sources are also needed [7]. In previous studies[8], the reduction of band gap energy was carried out by adding certain dopants to anatase crystals. Several types of dopants commonly used in this technique are transition metals, nitrogen, and oxygen [9], which are economically not very attractive and pose new problems to the environment due to the use of the metals.

An interesting development has been published in which the TiO_2 band gap was successfully reduced by using zeolite doping based on kaolin clay minerals [10]. Some of the advantages of this new method are that it is very economical, because clay is easy to find, the process is much simpler than that of doping with nitrogen and carbon and gives comparable degradation results. Santos et al, 2016 reported that clay has a more complete elements to lower energy of TiO_2 band gap with a simpler preparation process compared to doping with nitrogen and carbon and even gives better degradation results. Another development to improve the catalytic performance of semiconductor photocatalysts has been made by increasing the specific surface area of the catalyst [11]. The manufacture of porous TiO_2 using chitosan was successful in reducing the band gap energy to 3.00 eV but a new problem is the relatively low degradation efficiency to around 60 % [12] which is still low compared to the percent degradation in general. TiO_2 nanotubes which has lower band gap energy 2.54 eV [13].

Based on all the explanations above, in this article, we report the manufacture of titania composited with zeolite. The essence of this research is that the zeolite used is produced from materials that are cheap and easy to obtain because it is a combination of clay and rice husk ash.

Experiment

Materials. The materials used in this study were clay samples obtained from Padang Pariaman (West Sumatra, Indonesia), distilled water (H_2O), titanium dioxide (TiO_2) (Powder Anatase 25, Sangyo Kaisha Ltd.), rice husks, sodium hydroxide (NaOH) (Merck-Pro Analyst), pH paper, and 0.1 M hydrochloric acid (HCl).

Tools. The equipment used in this study were some standard glassware such as beakers, measuring flasks, test tubes, measuring cups, dropper pipettes, and funnels. Other equipment such as mortar and pestle, petri dish, oven, furnace, analytical balance, hotplate stirrer, shaker, autoclave, filter paper, and aluminum foil. While the instruments used are X-ray Fluorescence (XRF) (PAN Analytical Epsilon 3), X-ray Diffraction (XRD) (X'Port PAN Analytical), Fourier Transform Infra Red (FT-IR) (Thermo Scientific: Nicolet iS10), and the UV-Vis Diffusion Reflectance Spectrophotometer (UV-Vis DRS) (Analytic Jena).

Methodology

Clay thermal preparation and activation.

Clay samples were taken in Kalampayan, Pariaman, Padang Pariaman, West Sumatra. The samples were dried, then oven at 110°C for 3 hours. The resulting solid was mashed and then filtered and sieved so that it was ≤ 180μm in size. This result is designed as Heated-Clay (H-Clay). H-Clay is then calcined at 450°C for 4 hours and is designed as Calcinated-Clay (C-Clay). Samples were characterized by XRD and XRF.

Silica preparation from rice husk ash.

The rice husks are washed with water, then dried under sunlight. Then the rice husks were crushed to form husk ash using a grinder machine and calcined at a temperature of 600ºC for 3 hours. The resulting husk ash was then purified with 0.1 M HCl, namely, 10 mL for 1.0 gram of husk ash, stirring and boiling for 2 hours. After that, the sample was filtered with filter paper and washed with hot distilled water until the pH was neutral with pH universal indicator paper. The results were dried in an oven at a temperature of 105 °C for 4 hours. The silica obtained is in the form of a grayish white powder. The silica obtained is crushed, then 10 grams of husk ash are added 82.5 mL of 4N NaOH, then stirred with hot sauce over a hot plate. After thickening, The samples were transferred to a porcelain dish and melted at 500ºC for 1 hour. The result of this smelting is sodium silicate (Na_2SiO_3) cooled in the desiccator. The sodium silicate obtained is a white to grayish solid. The results were characterized by FTIR and XRF.

Zeolite synthesis (clay/rice husk ash).

The clay sample was weighed as much as 5.0 g, then added each 40 mL of 4N NaOH; and Na_2SiO_3 (sodium silicate) 10 % (w/v). The mixture was then put into an autoclave and heated in an oven at 40 °C for 24 hours. After that, the samples were reheated at 100 °C for 24 hours. The product is filtered with filter paper and washed with distilled water to neutral pH with pH universal indicator paper. Then the product was oven-dried at 120 °C for 6 hours, then calcined at 450 °C for 2 hours. Products were characterized by FTIR, XRD, and XRF.

Zeolite / TiO_2 preparation.

The sample of zeolite (clay-husk gray) was 90 % and TiO_2 10 % with a total amount of 5.0 grams, then added 40 mL of 4N NaOH and 10% (w / v) sodium silicate as much as 40 mL. The mixture was put into an autoclave and heated at 40 °C for 24 hours. After that the mixture was reheated in the oven at 100 °C for 24 hours. The product obtained was dried in an oven at 120 °C for 6 hours, then calcined at 450 °C for 2 hours. The results were characterized by XRD, XRF, FTIR, and UV-DRS.

Results and discussion

Characteristics of the Clay from Pariaman, Indonesia. H-Clay and C-Clay have physical characteristics as shown in Figure 1 where H-Clay is yellowish brown and after being calcined at 450 °C for 2 hours, the color changes to reddish brown. This indicates that there has been dehydration and decomposition of organic components accompanied by an increase in pH due to the release of some H^+ ions. pH can be measured by suspending the soil with water (1 : 1) after which the pH of the water on the surface is measured as soil pH [14]. Some literature explains that after going through the calcination process, many minerals from clay release their hydrates, such as Kaolin which turns into metakaolin and geotite into hematite [15; 16].

The H-Clay sample was modified with silica from rice husks in the form of sodium silicate solution (Na_2SiO_3) which aims to increase the Si/Al mole ratio, so that it can be converted into zeolite [17]. The Si/Al mole ratio of clay which generally ranges from 0.5–2.0 will be increased from 2.0 to 5.0 (intermediate zeolite) or it can be 5.0–100.0 (zeolite high) [18]. Based on the results of XRF (Tabel 1) H-Clay was chosen as the raw material for zeolite because it has a higher Si/Al mole ratio. In addition, Pariaman clay contains metals Si, Al, and Fe as the main elements and other elements as minority elements. The larger the Si/Al mole ratio of a clay, the clay tends to act as an adsorbent [8].

Fig. 1. Characteristics of Pariaman clay before and after calcination

Meanwhile, the smaller the Si/Al ratio of a clay, the clay is more likely to be active as a catalyst [19].

Journal of Chemistry and Technologies, 2022, *30*(1), 60-68

Table 1

XRF results of C-clay and H-clay samples

Element	h-Clay (% Elements)	c-Clay (%Elements)
Mg	0.285	0.261
Al	28.5	29.7
Si	51.9	51.6
K	0.794	0.767
Ca	0.335	0.279
Ti	1.31	1.23
Fe	15.5	14.8
Rb	0.520	0.491
Sr	0.458	0.475
Ba	0.398	0.397

From the XRD analysis (Figure 2), it can be explained that Pariaman clay is a polycrystalline consisting of illite (ICSD #90144), kaolinite (ICSD #84263), and quartz (ICSD #79635). This is common because the clay samples taken are of a non-living nature [20]. The most dominant mineral in this sample is quartz with the highest diffraction intensity. The thermal stability of H-clay and C-clay was studied from the XRD analysis results. Figure 1 shows that calcination of the material at 450°C does not appear to have an effect on the crystallinity of the sample. The crystallinity of the two samples, both H-clay and C-clay, was almost unchanged and there was no visible structural damage due to the influence of heat, which was indicated by the intensity retention of each main peak of the structure of the two materials, so it can be concluded that the two samples were thermally stable.

Synthesis and characterization of sodium silicate from rice husk ash.

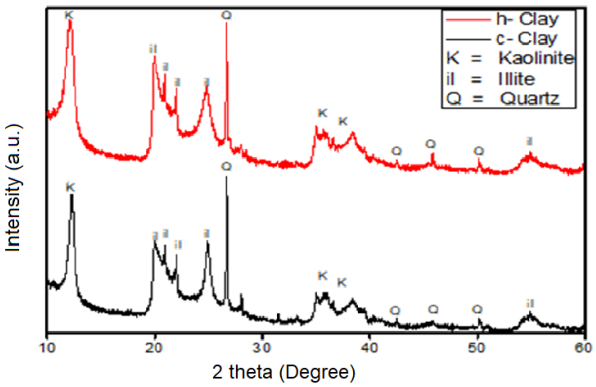

Fig. 2. XRD results of C-clay and H-clay samples

Rice husk ash in this study was used as a raw material in the synthesis of sodium silicate (Na_2SiO_3) which was carried out in 3 stages. The first step begins with the isolation of silica from rice husk ash by calcining the husks at a temperature of 600 °C for 3 hours, followed by purification of the silk using hydrochloric acid (HCl) solution. Washing with HCl aims to dissolve other oxides besides SiO_2 in the form of metal oxides such as MgO, K_2O, and Ca_2O [21]. The use of HCl in the purification process is due to the chemical nature of SiO_2 being insoluble/reactive to all acids except HF, so it does not reduce the yield of SiO_2 formed. Pure silica was then dissolved in NaOH and melted at 500°C. Melting at a temperature of 500°C is based on consideration of the melting point of NaOH, which is 318°C so that at that temperature NaOH dissociates completely to form Na^+ and OH^- ions. The choice of NaOH is because NaOH has a lower melting point than Na_2CO_3, which is 851°C, thus facilitating the formation of sodium silicate at a temperature that is not too high. The temperature used is based on the consideration that the melting point of NaOH is 318°C, so at that temperature it is expected that Na^+ ions and OH^- ions are completely formed as a result of the NaOH dissociation process [22]. The digestion which is followed by dissolving and smelting also aims to make the husk ash completely change into Na_2SiO_3. The sodium silicate obtained is a grayish-white solid which is then analyzed by FTIR and XRF.

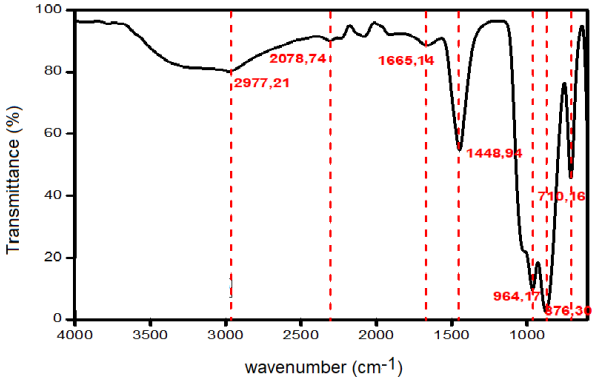

Fig. 3. Infrared spectrum, synthesis of sodium silicate

The resulting product was analyzed by FTIR (Figure 3) and XRF (Table 3). FTIR analysis was carried out to see the appearance of a very significant absorption band at a wave number of 964.17 cm-1 in the form of Si-O-Na stretching

vibrations, which proves that the sodium silicate compound has been successfully synthesized.

Table 2

Some of the important vibrations associated with sodium silicate

Wave Number (cm^{-1})	Observed Functional Groups	Transimitant (%)	Reference
2977.21	–OH groups Silanol (Si- OH) and H2O	80.24	Linda Trivana, 2015
2078.74	H-Si-Si-H	91.49	Fauzan et al, 2013
1665.14	Bending Vibration –OH of Silanol (Si-OH)	88.59	Fauzan et al, 2013
1448.94	Vibration Bending of Cylanol (Si-OH)	54.68	Fauzan et al, 2013
964.17	Si-O-Na (Stretching)	9.63	Linda Trivana, 2015
876.30	Si-O Group of Si-O-Si Bond	2.73	Fauzan et al, 2013
710.16	Symmetrical Stretch Vibration of Si-O to Siloxane (Si-O-Si)	45.75	Fauzan et al, 2013

The synthesized sodium silicate was also characterized by XRF. It aims to analyze the elements contained therein and also calculate the Si : Na ratio. The XRF results of sodium silicate are shown in table 3.

Table 3

The elemental composition of the synthesized sodium silicate

Element	% Element
Na	49.4
Si	47.4
K	1.43
Ca	1.77

XRF results showed that the synthesized sodium silicate contained Si and Na as the main elements with other elements as minor elements. This is supported by the Si:Na ratio of 1.6 : 2.2. The sodium silicate that has been successfully synthesized is used as a source of silica in the synthesis of zeolite in the next stage.

Synthesis and characterization of zeolites

The raw material used to synthesize zeolite is H-Clay, because it has the main component consisting of silica and alumina so that it can be used as a zeolite framework [23]. H-Clay also has a higher Si/Al mole ratio than C-Clay, so it is chosen to be the precursor. The synthesis of this zeolite requires a Si/Al mole ratio of 2.0–5.0, but from the results of the XRF H-Clay analysis in Table 1, the Si/Al ratio is only 1.756. Then the H-Clay was modified by adding an external source of silica, namely sodium silicate (Na_2SiO_3) which was processed from rice husk ash.

The H-clay obtained was dissolved in NaOH and Na_2SiO_3. NaOH solution plays a role in the activation of Si and Al in h-Clay into soluble minerals, namely sodium silicate and amorphous from alumina silicate. Both play a role in the formation of silica during the hydrothermal process. Meanwhile, Na_2SiO_3 solution acts as a source of additional silica apart from h-clay. Before the hydrothermal process, the mixture was heated at 40 °C for 24 hours, at this stage the formation of a crystal nucleus occurred and followed by completing the crystal formation at 100 °C for 24 hours [24].

The synthesized zeolite was washed with distilled water to neutral pH with the help of universal pH indicator paper. This aims to remove the residue that is not part of the zeolite formation, then the zeolite is dried so that the water trapped in the zeolite crystal pores evaporates. Zeolite characterization with the aid of X-ray diffraction was carried out at an angle range of 5–80°. It is used to identify the types of zeolite minerals they contain and their crystallinity [25].

The diffraction peaks obtained from the measurement data were matched with the X-ray diffraction standard, the Inorganic Crystal Structure Database (ICSD). The XRD results of the zeolite samples are shown in Figure 4 and show that the zeolite formed is a mixture of zeolites, consisting of zeolite P1, faujasite, zeolite X, Sodalite, and Nu-6. The XRD results for each sample were analyzed by comparing the angle of 2θ of the sample with 2θ of the ICSD data.

Linda Trivana et al. 2013, succeeded in synthesizing zeolite X from rice husk ash with metakaolin. In general, zeolites that are synthesized with rice husk ash percursors and clay minerals will form zeolite X. Many zeolites are formed because they are based on the nature of zeolite X which is thermodynamically unstable [9].

XRD characterization results based on ICSD data, for Sodalite (ICSD # 417676), X (ICSD # 99718), P1 (ICSD # 9550), Faujasite (ICSD # 416357), and nu-6 (ICSD # 413852).

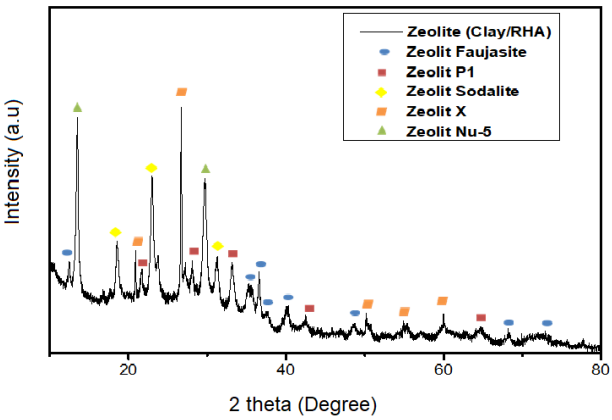

Figure 4. XRD patterns of synthesized zeolite

The peak is dominated by zeolite X and faujasite, but the highest intensity is found by zeolite X. This is supported by a theory and experiment which shows that zeolite synthesized from rice husk ash with clay, will generally form zeolite X which is more dominant. This zeolite plays an important role in the adsorption process and expands the surface of the clay-based TiO_2/ zeolite composite material. So that applications in the photodegradation process will run better [26].

Table 4

The elemental composition of the synthesized zeolite

Element	wt %
Al	23.6
Si	53.7
Ti	0.987
Na	6.46
Fe	12.2
Ca	1.612
K	1.441

Zeolites were also characterized by XRF to determine the success or failure of the modified clay [27]. In Table 4, it is found that the Si/Al ratio of the zeolite synthesized has increased, where the ratio found has increased from 1.76 to 2.20. This proves that zeolite have been successfully formed in terms of the Si/Al ratio (proven in the constituent material by XRD analysis). Silica modification is widely used to increase the ability of the material in adsorption properties. This will be a fairly good parameter in degrading pollutants and remediating the environment [28].

Synthesis and characterization of zeolite / TiO_2 composites

The zeolite/TiO_2 composite synthesis follows the conditions of the zeolite sample synthesis. The diffraction pattern of the zeolite/TiO_2 composite sample in Figure 5 shows that TiO_2 peaks (ICSD #158779) appear but in a fairly small intensity. This is because the TiO_2 is composited with a concentration of only 5 % (w/w). the 2θ angle of the zeolite/TiO_2 and ICSD composites was shown at 25.46°. The presence of TiO_2 on the diffractogram indicates the formation of a zeolite/TiO_2 composite synthesis.

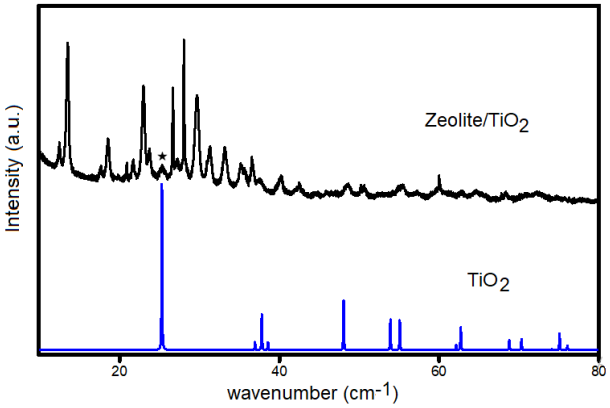

Figure 5. XRD results of zeolite/TiO_2 composites

The addition of TiO_2 aims to obtain a material with multiple benefits as an adsorbent-photocatalyst [29]. The synthesis of zeolite/TiO_2 composites using NaOH and Na_2SiO_3 under the same synthesis conditions as the zeolite synthesis described above. The reason for TiO_2 used is only 5% refers to the research of [4], that the amount of TiO_2 has no effect on the quality of later photocatalysts. This shows that this composite material will be more economical because TiO_2 is used only a little as a photocatalyst agent.

Table 5

The XRF result of Zeolite/TiO_2 composites

Element	% Element
Al	21.7
Si	47.3
Ti	7.41
Na	9.04
Fe	11.3
Ca	1.753
K	1.497

FTIR analysis is shown in Fig. 7, while XRF is shown in Table 5 which explains that there is an increase in the amount of Titanium in the

sample. Meanwhile, the Si/Al ratio of the composite is 2.10. This shows an increase as a result of using the same method as the previous zeolite synthesis.

The composite formed has a band gap value of 2.56 eV according to the Kubelka-Munkcalculation theory. This measurement is carried out with the UV-Vis DRS instrument, as described in Figure 6. This measurement aims to determine the band gap value of the material, so that it is known what rays are suitable for degradation at a later stage. With a band gap value of 2.56 eV, it is concluded that the work can be done in visible light. This is according to the calculation of the Planck formula.

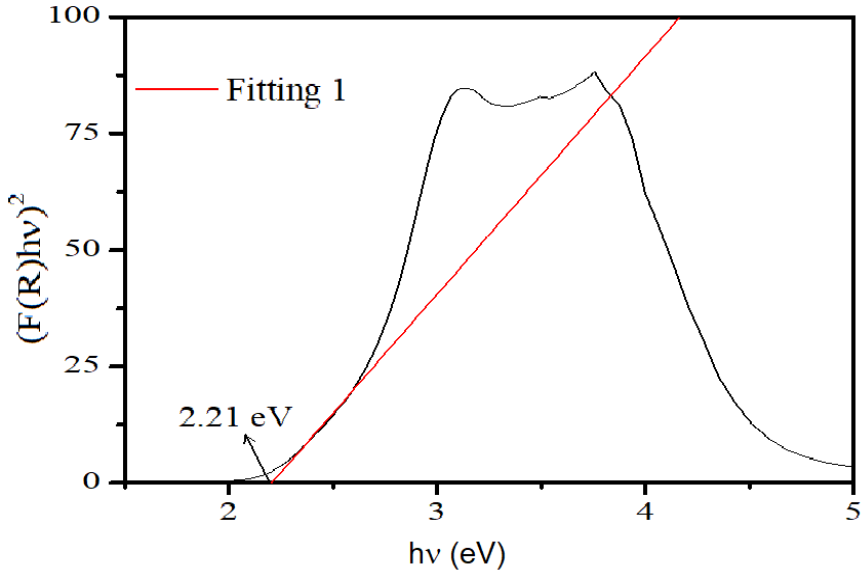

Figure 6. Analysis of Kubelka-Munk band-gap zeolite/TiO_2 composites

The theoretical TiO_2-anatase compound has a band gap value of 3.2 eV. Meanwhile, after being composited with zeolite derived from clay, there was a significant decrease in the band gap. This might occur due to the minerals in the clay that also adsorbed during the UV-Vis DRS measurement [1]. From this data it can be concluded that this composite material can be employed under sunlight. This is an advantage because the degradation process will be carried out more efficiently because the energy source is only visible light.

Identification of functional groups in zeolites is very important in the synthesis process to detect Si-O-Al bonds in samples because it can provide information related to minerals contained in clay that has been modified with rice husk ash. Figure 7 (a) shows the infrared spectra of the clay modified with rice husk ash. The wide peak at a frequency of 3397.95 cm^{-1} 1651.20 cm^{-1} refers to the OH^- stretched and OH^- bending molecular bonds, whereas at 1443.23 cm^{-1}, 555.55 cm^{-1} and 465 cm^{-1} indicate the T-O-T structure where T is Si or Al.

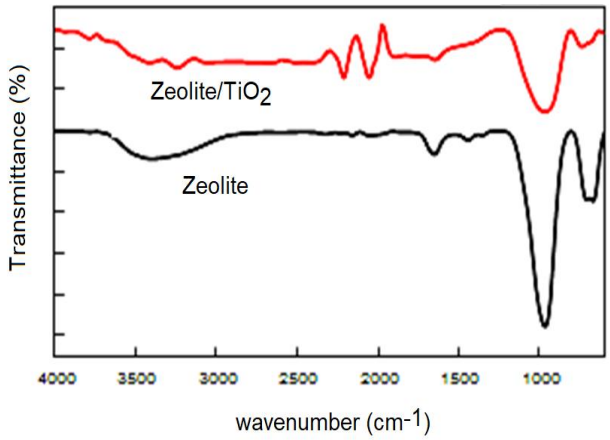

Fig. 7. FTIR spectra analysis (a) Zeolite and (b) Zeolite/TiO_2 composites

Based on Figure 7 (b) zeolite spectra in the composite, there is absorption at wave numbers 1645.73 cm^{-1} and 738.29 cm^{-1} which are external asymmetric and asymmetric strain absorption O-Si-O or O-Al-O. The absorption at wave number 966.40 cm^{-1} is a characteristic of Al-O and Si-O bonds. The presence of TiO2 on the zeolite surface is evidenced by the appearance of absorption at wavelengths of 2211.68 cm^{-1}, 2058.06 cm^{-1} and 1391.67 cm^{-1}, which are characteristics of the interference TiO_2.

Conclusion

A zeolite material has been successfully synthesized from rice husk ash and natural clay from Pariaman. This is evidenced from XRF analysis, where the Si/Al mole ratio is in the range of zeolite minerals. Then XRD analysis proved the diffraction peaks of several zeolite minerals consisting of faujasite, P1, sodalite, X, and nu-6. FTIR analysis showed that the zeolite which had been synthesized with clay and rice husk ash was successfully composed with TiO_2. Measurements with UV-DRS proved that the combination of zeolite with TiO_2 can change the TiO_2 gap energy from 3.20 eV to 2.56 eV which is suitable for applications in visible light.

Acknowledgement

Syukri et al thank FMIPA Andalas University for funding this research through research contract number 15/UN.16.03.D/PP/FMIPA/ 2020.

Reference

[1] Santos, L.R., Artur, J.S.M., Luciana, A.S. (2016). Preparation And Evaluation Of Composite With A Natural Red Clay And TiO_2 For Dye Discoloration Assisted By Visible Light. *Applied Clay Science*, 135. doi: 10.1016/j.clay.2016.11.002

[2] Angelia, Selvi Rina. (2014). Sintesis dan Karakterisasi Komposit Fotokatalis TiO_2 Anatase dan Rutil dengan Zeolit Alam Teraktivasi serta Uji Aktifitasnya pada Reaksi Esterifikasi Minyak Goreng Bekas. *Skripsi,* 10630010.

[3] Yang, Menjin. (2012). Band Gap Engineering and Carrier Transport In TiO_2 For Solar Energy Harvesting. *Skripsi University of Pittsburgh.*

[4] Setthaya, N., C. Prinya., S. Yin., P. Kedsarin. (2017). TiO_2-Zeolit Photocatalysts Made Of Metakaolin And Rice Husk Ash For Removal Of Methylene Blue Dye. *Powder technology*, 313, doi: 10.1016/j.powtec.2017.01.014

[5] Saravanan, R., Aviles, J., Gracia, F., Mosquera, E., Gupta, V. K. (2018). Crystallinity And Lowering Band Gap Induced Visible Light Photocatalytic Activity Of TiO_2/CS (Chitosan) Nanocomposites. *International Journal of Biological Macromolecules*. 109, 1239–1245.

[6] Choudhury, B. , Bayan, S., Choudhury, A., Chakraborty, P. (2016). Narrowing Of Band Gap And Effective Charge Carrier Separation In Oxygen Deficient TiO_2 Nanotubes With Improved Visible Light Photocatalytic Activity. *Journal of Colloid and Interface Science*. 465. 1–10.

[7] Liu, X., Liu, Y, Lu, S., Guo, W., Xi, B. (2018). Performance And Mechanism Into TiO_2/Zeolite Composites For Sulfadiazine Adsorption And Photodegradation. *Chemical Engineering Journal*. 350, 131–147

[8] Trivana, L. (2013). Sintesis dan Karakterisasi Sintesis Zeolit X Dan Komposit Zeolit/TiO_2 Dari Kaolin Dengan Sekam Padi Sebagai Sumber Silika. *Skripsi.*

[9] Nitya, V. N. C. (2012). Degradasi Limbah Deterjen (Senyawa Linear Alkilbenzen Sulfonat) Dengan Fotokatalis Komposit Berbasis TiO_2 dan Batu Apung. *Skripsi.*

[10] Mishra, A., Mehta, A., Basu, S. (2018). Clay Supported TiO_2-Nanoparticles For Photocatalytic Degradation Of Environmental Pollutants: A Review. *Journal of Environmental Chemical Engineering, 6*(5), 6088-6107. https://doi.org/10.1016/j.jece.2018.09.029

[11] Beata, Szczepanik. (2008). Photocatalytic Degradation Of Organic Contaminants Over Clay-TiO_2 Nanocomposites: A Review. *Applied Clay Science.* 141:227.

[12] Poluokan, Michell.; Wuntu, Adi.; Sangi, Meiske. (2015). Aktivitas Fotokatalitik TiO_2 – Karbon Aktif dan TiO_2–Zeolit pada Fotodegradasi Zat Warna Remazol Yellow . *Jurnal Mipa Unsrat Online 4*, 2, 137–140.

[13] Fuadi, A. M., Musthofa, M. Harismah, K., Haryanto, Hidayati, N. (2012). Pembuatan Zeolit Sintetis Dari Sekam Padi. *Simposium Nasional RAPI XI FT UMS*.

[14] Sani, A. Arfan., Atiek, R. N., Diana, R. (2009). Pembuatan Fotokatalis TiO_2-Zeolit Alam Asal Tasikmalaya Untuk Fotodegradasi *Methylene Blue*. *Jurnal Zeolit Indonesia*, *1*(8), 6–14.

[15] Fadlullah, M. (2014). Pengaruh Variasi Rasio Si/Al pada Sintesis Zeolit dengan Metode Refluks. *Jurnal Kimia Sains dan Aplikasi*, *17*(3), 100 – 103

[16] Saeed, M., Muneer, M., Akram, N., Ul Haq, A., Afzal, N., Hamayun, M. (2019). Synthesis And Characterization Of Silver Loaded Alumina And Evaluation Of Its Photo Catalytic Activity On Photo Degradation Of Methylene Blue Dye. *Chemical Engineering Research and Design,* 148: 218–226.

[17] Mirmasoomi, S. R., Ghazi, M. M, Galedari, M. (2016). Photocatalytic Degradation Of Diazinon Under Visible Light Using TiO_2 /Fe_2O_3 Nanocomposite Synthesized By Ultrasonic-Assisted Impregnation Method. *Separation and Purification Technology,* 175,418–427.

[18] Ahmad, A. F., Risanti, D. D., Mawarni, L. J. (2013). Sintesis Natrium Silikat Dari Lumpur Lapindo Sebagai Inhibitor Korosi. *Jurnal Teknik POMITS*. *2*, 2.

[19] Aichun, W., Duoxiao, W., Chao, W., Xudong, Z., Zhangsheng, L., Peizhong, F., Xuemei, O., Yinghuai, Q., Hermenegildo, G., Jinan, N. (2019). A Comparative Photocatalytic Study Of TiO_2 Loaded On Three Natural Clays With Different Morphologies. *Applied Clay Science*. 183.

[20] Hadjltaief, H. B., Maria, E. G., Mourad, B. Z., Da Costa, P. (2014). TiO_2/Clay As A Heterogeneous Catalyst In Photocatalytic/Photochemical Oxidation Of Anionic

Reactive Blue 19. *Arabian Journal of Chemistry, 12*(7), 1454–1462. https://doi.org/10.1016/j.arabjc.2014.11.006

[21] Mishra, A., Mehta, A., Sharma, M., Basu, A. (2017). Enhanced Heterogeneous Photodegradation Of VOC And Dye Using Microwave Synthesized TiO_2/Clay Nanocomposites: A Comparison Study Of Different Type Of Clays. *Journal of Alloys and Compounds.* 694, 574-580.

[22] Wang, C., Shi, H., Zhang, P., Li, Y. (2011). Synthesis And Characterization Of Kaolinite/TiO_2 Nano-Photocatalysts. *Applied Clay Science*. 53, 646–649.

[23] Todorova, N., Giannakopouloua, T., Karapati, S., Petridis, D., Vaimakis, T., Trapalis, C. (2014). Composite TiO_2/Clays Materials For Photocatalytic NOx Oxidation. *Applied Surface Science*, 319, 113–120. https://doi.org/10.1016/j.apsusc.2014.07.020

[24] Zhoua, F., Yana, C., Wang, H., Zhou, S. (2017). Komarneni. Sepiolite-TiO_2 Nanocomposites For Photocatalysis: Synthesis By Microwave Hydrothermal Treatment Versus Calcination. *Applied Clay Science.* 146, 246–253.

[25] Gombos, E.D., D. Krakkó, G, Záray, Á. llésa, S. Dóbéa, Szegedia, Á. (2020). Laponite Immobilized TiO_2 Catalysts For Photocatalytic Degradation Of Phenols. *Journal of Photochemistry & Photobiology A: Chemistry*. 387.

[26] Huang, S., Lua, X., Lia, Z., Ravishankara, H., Wanga, J., Wang X. (2018). A Biomimetic Approach Towards The Synthesis Of Tio2/Carbon-Clay As A Highly Recoverable Photocatalyst. *Journal of Photochemistry and Photobiology A: Chemistry* 351, 131–138.

[27] Dong, Z., Ling, M., Jiang, Y., Han, M., Rena, G., Zhang, J., Ren, X., Li, F., Xue. B. (2019). Preparation And Properties Of TiO_2/Illite Composites Synthesized At Different Hydrothermal pH Values. *Chemical Physics*. 525.

[28] Belessi, V., Lambropoulou, D., Konstantinou, I., Katsoulidis, A., Pomonis, P., Petridis, T. (2007). Albanis. Structure And Photocatalytic Performance Of TiO_2/Clay Nanocomposites For The Degradation Of Dimethachlor. *Applied Catalysis B: Environmental*. 73, 292–299.